ORIGINAL RESEARCH

Encapsulation of plasmid DNA in calcium phosphate nanoparticles: stem cell uptake and gene transfer efficiency

Xia Cao*
Wenwen Deng*
Yuan Wei*
Weiyan Su
Yan Yang
Yawei Wei
Jiangnan Yu
Ximing Xu

Department of Pharmaceutics, School of Pharmacy, and Center for Nano Drug/Gene Delivery and Tissue Engineering, Jiangsu University, Jingkou District, Zhenjiang, People's Republic of China

*These authors contributed equally to this work

Correspondence: Ximing Xu; Jiangnan Yu
Department of Pharmaceutics, School of Pharmacy, Jiangsu University, Zhenjiang 212001, People's Republic of China
Tel +86 511 8503 8451
Fax +86 511 8503 8451
Email xmxu@ujs.edu.cn; yjn@ujs.edu.cn

Background: The purpose of this study was to develop calcium phosphate nanocomposite particles encapsulating plasmid DNA (CP-pDNA) nanoparticles as a nonviral vector for gene delivery.

Methods: CP-pDNA nanoparticles employing plasmid transforming growth factor beta 1 (TGF-β1) were prepared and characterized. The transfection efficiency and cell viability of the CP-pDNA nanoparticles were evaluated in mesenchymal stem cells, which were identified by immunofluorescence staining. Cytotoxicity of plasmid TGF-β1 and calcium phosphate to mesenchymal stem cells were evaluated by MTT assay.

Results: The integrity of TGF-β1 encapsulated in the CP-pDNA nanoparticles was maintained. The well dispersed CP-pDNA nanoparticles exhibited an ultralow particle size (20–50 nm) and significantly lower cytotoxicity than Lipofectamine™ 2000. Immunofluorescence staining revealed that the cultured cells in this study were probably mesenchymal stem cells. The cellular uptake and transfection efficiency of the CP-pDNA nanoparticles into the mesenchymal stem cells were higher than that of needle-like calcium phosphate nanoparticles and a standard calcium phosphate transfection kit. Furthermore, live cell imaging and confocal laser microscopy vividly showed the transportation process of the CP-pDNA nanoparticles in mesenchymal stem cells. The results of a cytotoxicity assay found that both plasmid TGF-β1 and calcium phosphate were not toxic to mesenchymal stem cells.

Conclusion: CP-pDNA nanoparticles can be developed into an effective alternative as a nonviral gene delivery system that is highly efficient and has low cytotoxicity.

Keywords: calcium phosphate nanoparticles, transfection, gene delivery, cellular uptake, mesenchymal stem cells

Introduction

Gene therapy, ie, delivery of therapeutic nucleic acids to target cells to replace a missing or defective gene, has emerged as an alternative treatment of acquired or inherited genetic disorders currently considered incurable, such as cancer,[1,2] diabetes,[3] and hemophilia.[4] Because naked DNA can scarcely penetrate most cell membranes before being degraded by nucleases, effective gene carriers or vectors that do not cause vector-associated toxicity are highly desirable.[5] To achieve this objective, both viral and nonviral gene vectors have been widely investigated. Among these carriers, viral vectors[6] appear to be the most effective because of the natural tendency of viruses to infect cells. However, these viral vectors have significant shortcomings, such as an immune response against the transfection system, cancer induction, poor target specificity, and a low capacity to incorporate exogenous genes,[7,8] that limit their application in gene therapy.

Therefore, it is highly desirable to design and fabricate a safe and effective nonviral gene delivery vector. Nonviral gene vehicles have been undergoing intensive research due to several advantages over viral carriers, such as biocompatibility and biodegradability, a lack of immunogenicity, negligible toxicity, the ability to carry large therapeutic genes, and a reduced production cost.[9] Currently, the most commonly used nonviral vectors are complexes composed of plasmid DNA and cationic lipids or cationic polymers. Nevertheless, cationic lipids and cationic polymers are accompanied by a number of drawbacks, such as their relatively large size and toxicity both in vitro and in vivo.[10]

In consideration of the stumbling blocks existing for both cationic lipids and cationic polymers, inorganic nanoparticles, such as metal and metal oxide nanoparticles,[11–13] carbon nanotubes,[14] and calcium phosphate nanoparticles,[15] have emerged as alternatives due to their versatile properties suitable for cellular delivery, which include wide availability, rich functionality, biocompatibility, the potential capacity of target delivery, and the controlled release of the carried DNA. As one of the most commonly used inorganic materials in biochemistry and biotechnology, calcium phosphate nanoparticles enjoy several inherent properties that set this system apart for gene delivery. Unlike metal and metal oxide nanoparticles which are difficult to prepare,[13] and carbon nanotubes which are limited by safety issues in biomedical applications,[16] calcium phosphate has excellent biocompatibility because it can be found throughout the body in the form of amorphous calcium phosphate and crystalline hydroxyapatite, which is the major component of bone and tooth enamel. Additionally, reasonably high but benign concentrations of Ca^{2+} and PO_4^{3-} (1–5 mM) occur in all vertebrates and are naturally nontoxic as well as bioresorbable.[17] Moreover, the solubility of calcium phosphate is variable, as regulated by the kidney.[18] This natural occurrence of calcium phosphate is one of its primary advantages over other synthetic gene delivery systems.

In the last decade, calcium phosphate-DNA nanoparticles have been widely investigated to transfect different kinds of cell lines. Several developments have been reported regarding calcium phosphate particles encapsulating therapeutic nucleic acid and transfecting it into liver cells,[19] fibroblasts,[20] osteoblasts,[21] tumor cells[22] and other cells. In one case, Roy et al[23] prepared ultralow size (80 nm) calcium phosphate-DNA nanoparticles with a modified p-amino-1-thio-β-galactopyranoside ligand, and these calcium phosphate-DNA nanoparticles were then used as nonviral vectors for β-galactopyranoside receptor-targeted

gene delivery. Bisht et al[24] synthesized nanoparticles of calcium phosphate encapsulating plasmid DNA which were used to transfect HeLa cell lines, and the results displayed higher transfection efficiency than that of the commercial transfecting reagent, Polyfect™. They also reported that calcium phosphate nanoparticles can be carried across the cell membrane via calcium ion channel-mediated endocytosis. In another study reported by Liu et al,[25] when calcium phosphate nanoparticles combined with suicide genes yCDglyTK for nasopharyngeal carcinoma therapy in vitro, just 24.76% of cells survived when the wild-type CNE-2 cells were treated with the calcium phosphate nanoparticle-yCDglyTK complex plus the prodrug, 5-FC (200 mg/mL), indicating that calcium phosphate nanoparticles might be a potential vector for gene therapy. More recently, more and more attention has been focused on calcium phosphate nanoparticles for gene delivery, resulting in wider and deeper application of calcium phosphate in the field of gene therapy. Zhang et al[26] synthesized PEGylated calcium phosphate nanocomposites which were used as smart environment-sensitive carriers for siRNA delivery. Furthermore, calcium phosphate-DNA nanoparticles could also be employed together with alginate hydrogels to induce in vivo osteogenesis, as reported by Krebs et al.[27]

The technique of calcium phosphate coprecipitation for in vitro transfection is used as a routine laboratory procedure and relies heavily on divalent metal cations, such as Ca^{2+}, Mg^{2+}, Mn^{2+}, and Ba^{2+}, forming ionic complexes with the helical phosphates of DNA.[23] Therefore, calcium phosphate forms complexes with the nucleic acid backbone. Traditionally, amorphous calcium phosphate particles can be formed in a relatively straightforward precipitation reaction. For instance, mixing a calcium chloride solution containing DNA and a phosphate-buffered saline solution results in precipitates consisting of calcium phosphate and DNA.[28] However, the calcium phosphate nanoparticles prepared by these schemes are relatively large (greater than 100 nm) and have significant agglomeration.[29] These shortcomings have severely handicapped the process of cellular uptake after transfection, leading to decreased transfection efficiency.

Taking these problems into consideration, many researchers have been attempted to prepare ultralow-sized calcium phosphate nanoparticles entrapping DNA molecules. Liu et al[25] reported a scheme to prepare calcium phosphate nanoparticles ranging from 24 to 35 nm in size and coated with bovine serum albumin as an efficient gene carrier in cancer gene therapy. Pedraza et al[30] have conducted a series of comprehensive investigations on the physicochemical

characteristics of calcium phosphate nanoparticles, which are the factors affecting transfection efficiency, and found that the key parameters for effective calcium phosphate nanoparticle transfection were an optimal concentration of calcium and chloride ions and a nanosized nonagglomerated precipitate. Recently, several researchers[29,31,32] encapsulated organic dyes into calcium phosphate nanocomposite particles for intracellular imaging and drug delivery to cells. In these studies, researchers developed a new strategy to produce ultralow sized and well dispersed calcium phosphate nanocomposite particles.

Enlightened by these previous studies, we herein constructed calcium phosphate nanoparticles incorporating plasmid transforming growth factor beta 1 (TGF-β1), which are ultrasmall and show excellent dispersion in medium. These plasmid-loaded calcium phosphate nanoparticles were subsequently used to transfect mesenchymal stem cells from rat femur marrow. To the best of our knowledge, although calcium phosphate nanoparticles have been employed to transfect many kinds of cells, their application as a gene vector for direct mesenchymal stem cell transfection has rarely been reported. Mesenchymal stem cells are a promising alternative for use in gene therapy due to their strong capabilities of self-renewal and differentiation into various types of cells.[33] The functional cytokine TGF-β1 encoded by the plasmid was introduced in the current study due to its favorable properties in gene therapy.[34]

Materials and methods
Materials
The nonionic surfactant poly (oxyethylene)-nonylphenyl ether (Igepal CO-520) cyclohexane and silane-coupling agent 3-aminopropyltriethoxysilane (APS) were purchased from Sigma-Aldrich (St Louis, MO). Glacial acetic acid and absolute ethanol were obtained from Chemical Reagent Co, Ltd, of China National Pharmaceutical Group and were used without further purification. All of the aqueous stock solutions were prepared with deionized water. Silica spheres (50 μm in size, 60 Å in pore size) were purchased from Sepax Technologies (Newark, DE). Fetal bovine serum, Dulbecco's modified Eagle's medium (DMEM), penicillin, streptomycin, and trypsin were obtained from Gibco-Invitrogen (Grand Island, NY). The standard calcium phosphate transfection kit and other chemicals were obtained from Beyotime Biotechnology (Jiangsu, China), except when otherwise specified.

Rabbit antimouse CD13, CD44, CD106 antibodies, sheep antirabbit IgG labeled with Cy3, and vimentin antibody were purchased from Boston Corporation (Wuhan, China). TGF-β1 plasmid (Figure 1A) was kindly provided by Dr Guang-Jian Zhang at the Medical College of Wisconsin (Milwaukee, WI). Purified TGF-β1 plasmid was prepared with the Pure Yield Plasmid Midiprep Kit (Promega, Madison, WI). Propidium iodide and colchicine were supplied by the Beyotime Institute of Biotechnology (Shanghai, China). One-day-old male white Sprague-Dawley rats were supplied by the Experimental Animal Center of Jiangsu University. The animal experimental protocol was approved by the University Ethics Committee for the use of experimental animals and conformed to the Guide for Care and Use of Laboratory Animals.

Preparation of CP-pDNA nanoparticles in microemulsion
The preparation process for plasmid DNA-loaded calcium phosphate (CP-pDNA) nanoparticles followed a published report[29] with some modifications. Briefly, two separate microemulsions (A and B) were formed with a cyclohexane/Igepal CO-520/water system in which the cyclohexane acted as the oil phase reaction medium and Igepal CO-520 was the surfactant. In the first step, a 29% (v/v ratio) Igepal CO-520 solution in cyclohexane was prepared. Excessive water was then added to bring the total volume of water to 450 μL to adjust the molar ratio of water to Igepal CO-520 to 10. The results of previous trial tests showed that because both microemulsion A and B were of the water-in-oil type, when the molar ratio was over 10, the emulsion would be destroyed, and when the molar ratio was less than 10, there was excess surfactant (data not shown). Thus, the optimal molar ratio of water to Igepal CO-520 is 10. For the microemulsion A preparation, 2.94 μg of plasmid DNA in 70 μL of 1.36 mM calcium chloride was added to 25 mL of the above-mentioned Igepal CO-520 solution in cyclohexane. The mixture was stirred continuously for 2 minutes to form microemulsion A. Similarly, for microemulsion B, 2.94 μg of plasmid DNA in 70 μL of 0.35 mM disodium hydrogen phosphate and 50 μL of 0.2 M Tris-HCl buffer (pH 7.4) were added to 25 mL of Igepal CO-520 solution in cyclohexane. The mixture was stirred continuously for 2 minutes to form microemulsion B. The amount of plasmid DNA was determined according to the loading capacity results described below. The addition of the aqueous solution to the cyclohexane/Igepal CO-520 solution forms a self-assembled, reverse microemulsion suspension. Both of the microemulsions were optically clear solutions. Microemulsion B was added into microemulsion A at 20 drops per minute with
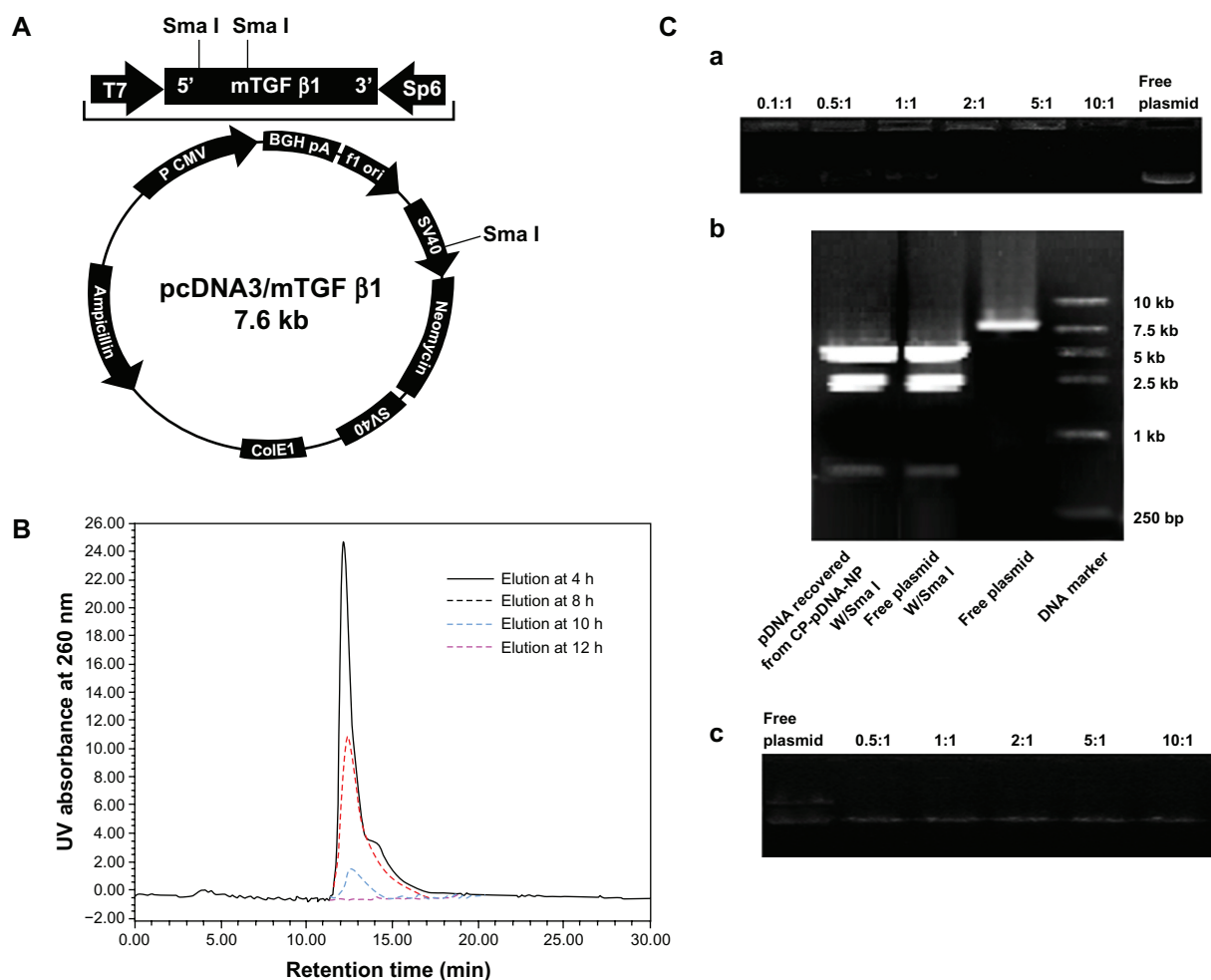
Figure 1 (**A**) Structure map of plasmid TGF-β1. (**B**) Ultraviolet high-pressure liquid chromatography analysis of CP-pDNA nanoparticles samples eluted with ethanol/water (70:30, v/v) solvent from the silica column. The samples were collected at 4, 8, 10, and 12 hours after elution started. Chromatography was detected at 260 nm. (**C**) Agarose gel electrophoresis of CP-pDNA nanoparticles. Panel a shows the plasmid DNA loading capacities of the CP-pDNA nanoparticles. DNA was detected with ethidium bromide in the gel. Free plasmid and CP-pDNA nanoparticles made with calcium phosphate/plasmid DNA ratios equal to 0.1:1, 0.5:1, 1:1, 2:1, 5:1, and 10:1 (from left side to right side) were tested. Panel b shows an assay of plasmid DNA integrity in the CP-pDNA nanoparticles. The plasmid DNA released from the CP-pDNA nanoparticles was digested with SmaI and evaluated on agarose gel. Lane 1 shows plasmid DNA recovered from the CP-pDNA nanoparticles digested with SmaI; lane 2 shows free plasmid DNA digested with SmaI; lane 3 shows free plasmid DNA; lane 4 shows the DNA marker. Panel c shows an assay of the topological structure of plasmid DNA released from the CP-pDNA nanoparticles.
Abbreviations: TGF-β1, transforming growth factor beta-1; CP, calcium phosphate; pDNA, plasmid DNA; Sma I, *Serratia marcescens I*; UV, ultraviolet.

continuous magnetic stirring at 4°C. The resulting microemulsion was allowed to undergo emulsion exchange for another 10 minutes with continuous stirring until complete translucency, during which time the doped calcium phosphate nanoparticles precipitated in the emulsions. Without adding dispersant, the CP-pDNA nanoparticle microemulsion was diluted by pH-adjusted absolute ethanol (pH 7.0) before van der Waals chromatography laundering.

Isolation of CP-pDNA nanoparticles

CP-pDNA nanoparticle isolation was performed using the van der Waals chromatography laundering method, modified from a published report.[29] Prior to the column preparation, silica spheres (50 μm, 60 Å) were pretreated with the

following steps: silica microspheres (90 g) were mixed with APS (0.336 mL), glacial acetic acid (1.5 mL), double-distilled water (7.5 mL), and absolute ethanol (150 mL). The spheres were stirred overnight and subsequently oven-dried at 70°C. The CP-pDNA nanoparticle microemulsion (50 mL) was diluted by absolute ethanol (pH 7.0, 150 mL) before loading onto the silica column. The silica column was prepared by packing APS-treated silica microspheres into an empty HR 5/5 column (Piscataway, NJ) and equilibrating with absolute ethanol before sample loading. The high-pressure liquid chromatography (HPLC) system used to isolate the CP-pDNA nanoparticles was the Waters HPLC system (Waters 510 HPLC Pump, Waters™ 486 tunable absorbance detector). The terminal end of the column was connected to a Waters

486 ultraviolet-visible spectrometer with a detector set at the wavelength of 260 nm. The suspension of CP-pDNA nanoparticles was pumped into the HPLC system followed by absolute ethanol as the washing solvent. The CP-pDNA nanoparticles were attracted to the stationary phase (the silica spheres) by van der Waals forces in the low dielectric media (absolute ethanol). The column was first washed with absolute ethanol (400 mL) to minimize the surfactant Igepal CO-520 concentration (less than 1×10^{-3} M) with the entire HPLC operation fixed at 0.5 mL/minute. During this process, the free plasmid DNA and the cyclohexane were completely removed (below the detection limits of the ultraviolet HPLC analysis). After ethanol washing, the nanoparticles, which remained on the column due to van der Waals attractive forces, were eluted with a 70:30 ethanol-water solution with NaCl (5×10^{-4} M, prepared with CO_2-free deionized water, pH 7) at a speed of 0.5 mL/minute for 12 hours. The eluted CP-pDNA nanoparticles in the 70:30 ethanol-water with NaCl (5×10^{-4} M) solution were concentrated by whirl-evaporation for 6 hours at 37°C and subsequently dialyzed with phosphate-buffered saline overnight at 4°C using a dialysis bag (with a cutoff molecular weight of 12 kDa, Biosharp, USA provided by Nanjing Super-bio Biotechnology Co, Ltd, Nanjing, China) to remove the NaCl. The final CP-pDNA nanoparticle solution within the dialysis bag was collected and stored at 4°C until use.

Determination of loading capacity, integrity, and topological structure

To determine the optimized plasmid DNA loading capacity of calcium phosphate nanoparticles, different amounts of TGF-β1 DNA (from 0.1 to 10 µg) were used to prepare CP-pDNA nanoparticle microemulsions, while the same amounts of calcium and phosphate ions (1 µg) were used for different preparations. The isolated CP-pDNA nanoparticle samples were dispersed in water and subsequently subjected to agarose gel electrophoresis. For each sample, 10 µL of nanoparticles were loaded onto a 1% agarose gel containing propidium iodide and electrophoresed at 100 V for one hour. If the calcium phosphate nanoparticles were oversaturated with plasmid DNA, the free plasmid DNA could be observed in the agarose gel. The CP-pDNA nanoparticles were centrifuged at 50,000 rpm for 15 minutes at 4°C. The pellet was dissolved in sodium acetate (pH 3.0). The TGF-β1 plasmid DNA could be released from the CP-pDNA nanoparticles because the calcium phosphate was sensitive to the mildly acidic conditions. The plasmid DNA was concentrated and subsequently subjected to SmaI digestion and agarose gel

electrophoresis. The integrity of the plasmid DNA was analyzed based on the results of the gel electrophoresis. Additionally, the topological structure of free plasmid DNA as well as plasmid DNA released from CP-pDNA nanoparticles with different weight ratios of calcium phosphate to plasmid DNA (0.5:1, 1:1, 2:1, 5:1, and 10:1) were also investigated via gel electrophoresis.

Transmission electron microscopy

Transmission electron microscopy (TEM) images were captured on a JEM-2100 instrument (JEOL, Tokyo, Japan). Briefly, one drop of the freshly prepared nanoparticle suspension was placed onto a carbon film grid with a copper backing and was self-dried at room temperature (25°C). The dried grid was then examined under the electron microscope.

Isolation and identification of mesenchymal stem cells

Bone marrow cells were harvested by flushing the tibia and femur of one-day-old male white Sprague-Dawley rats with DMEM supplemented with 10% fetal bovine serum. Nucleated cells were isolated from bone marrow cells with a density gradient Ficoll solution (GE Healthcare, Braunschweig, Germany) and subsequently resuspended in complete culture medium supplemented with penicillin 50 U/mL and streptomycin 50 mg/mL. The nucleated cells were incubated at 37°C in 5% humidified CO_2 for 12–14 days as the primary culture or until the formation of large colonies.

When large colonies developed to 80%–90% confluence, passage 3 cells were washed three times with phosphate-buffered saline and trypsinized with 0.25% trypsin in 1 mM EDTA for 5 minutes at 37°C. After centrifugation, the mesenchymal stem cells were resuspended in fetal bovine serum-supplemented medium and seeded in 24-well plates (Corning, NY) at a density of 5×10^4 cells per well (a density of 30,000 cells/ well) and were expanded to 80%–90% confluence (approximately 100,000 cells) before immunofluorescence staining. Briefly, the cells in each well were washed three times with 500 µL of phosphate-buffered saline and subsequently fixed in 500 µL of 4% paraformaldehyde for 4 hours. The primary antibodies CD13, CD44, CD106, CD34, CD71, and vimentin were diluted with phosphate-buffered saline at an antibody/ phosphate-buffered saline ratio of 1:100 (v/v) according to the manufacturer's instructions and were added into each well (300 µL/well) followed by an overnight incubation at 4°C. After incubation, the cells were washed three times with 500 µL of phosphate-buffered saline followed by the addition

of sheep-antirabbit IgG secondary antibody labeled with CY3 (300 µL/well) for one hour of incubation at room temperature. After washing with 500 µL of phosphate-buffered saline as described above, 300 µL of 5 µg/mL Hoechst 33342 was added to each well and incubated for 10 minutes at room temperature. Finally, the cells were washed with 500 µL of phosphate-buffered saline as described above and observed on a fluorescent microscope. After transfection, immunofluorescence staining was also conducted as described above to check if the stem cells had differentiated.

Transfection of mesenchymal stem cells with CP-pDNA nanoparticles

The mesenchymal stem cells were seeded 24 hours prior to the CP-pDNA nanoparticles transfection at a density of 2×10^5 cells per well on a 24-well plate. In each well, complete medium (500 µL, DMEM containing 10% fetal bovine serum and supplemented with 50 U/mL penicillin and 50 µg/mL streptomycin) was used. Immediately before the transfection, the number of living cell numbers for five different wells was calculated using trypan blue staining. The results demonstrated that there was approximately the same number of cells in each well. At the time of the transfection, the medium in each well was replaced with fresh complete medium (500 µL). The CP-pDNA nanoparticles were added into each well and incubated with the cells for 6 days. The medium in each well was replaced by fresh medium at 4 hours and 3 days after the transfection. Transfection with Lipofectamine 2000 was performed according to the manual (Invitrogen). The standard calcium phosphate transfection was carried out with a kit purchased from Beyotime Biotechnology. Another transfection method in which the plasmid DNA was mixed with preformed needle-like calcium phosphate nanoparticles was tested according to a published report.[35] All of the transfection experiments were performed with the same amount of plasmid (1 µg/well). The data are presented as the mean ± standard deviation (n = 5). The medium from the TGF-β1-transfected cell cultures was collected at 3 days and 6 days after transfection. The medium TGF-β1 concentrations (n = 5 for each treatment) were tested with a rat TGF-β1 enzyme-linked immunosorbent assay kit (USCN Life Science and Technology, Missouri City, TX). The medium from the untreated mesenchymal stem cell cultures was used for blank controls.

Cytotoxicity assay

The mesenchymal stem cells were seeded in 96-well plates and incubated for 24 hours before transfection. For each well, 0.2 µg of plasmid DNA was transfected as CP-pDNA nanoparticles, with Lipofectamine 2000 or as naked plasmid DNA. Different weight ratios (2:1 to 10:1) of calcium phosphate:pDNA and Lipofectamine 2000:pDNA were tested. Four hours later, the medium was replaced by 100 µL of fresh medium. After 3 days of incubation, the metabolic activities of the transfected cells were determined using a standard MTT (thiazolyl blue) assay. Moreover, the cytotoxicity of calcium phosphate to mesenchymal stem cells was evaluated as well. Mesenchymal stem cells were exposed to calcium phosphate with 400 ng per well up to 6 days. After that, cell viability was tested by MTT assay.

Live cell imaging and confocal laser microscopy

To observe the processing of CP-pDNA nanoparticles in the cells, propidium iodide was used as the marker of plasmid DNA. Propidium iodide was added to the microemulsions during the preparation of the nanoparticles. Time-lapse images of the cell morphology and movement were captured with a single 400 µm z-stack (15 mm slices) every 30 minutes for an 18-hour period. The pictures were taken under a Nikon TE 2000 PFS fluorescent microscope equipped with a motorized stage and an environmental sample chamber.

To investigate the mechanism of cellular uptake, culture medium containing 10 µg/mL colchicine was added when the CP-pDNA nanoparticles were transfecting the mesenchymal stem cells. After incubation for 4 hours, the transfection medium was replaced with serum-free DMEM medium with 10 µg/mL colchicine. Except for the addition of the colchicine, all of the transfection operation steps were the same. To observe nuclear transport, the mesenchymal stem cells transfected with propidium iodide-labeled free plasmid DNA, propidium iodide-labeled CP-pDNA nanoparticles, and propidium iodide-labeled CP-pDNA nanoparticles plus colchicine (CP-pDNA nanoparticles + colchicine) were loaded onto poly-L-Lys-coated slides, fixed with 4% formaldehyde (methanol-free, Polysciences Inc, Warrington, PA) in phosphate-buffered saline for 30 minutes and stained with Hoechst 33342 (0.5 ng/mL) in saline for 10 minutes. The fixative was then removed, and the cells were washed with phosphate-buffered saline to remove the formaldehyde. The slides were visualized with a confocal laser microscope (Zeiss LSM700, Gottingen, Germany) equipped with an inverted microscope (Axio Observer Z1, Zeiss) and four solid-state lasers (405, 473, 532, and 637 nm).

Statistical analysis

All of the values are represented as the mean ± standard deviation. The significant differences among different groups were tested using the Student's *t*-test and a one-way analysis of variance with a least significant difference post hoc test by the SPSS statistic software (SPSS version 15.0, SPSS Inc, Chicago, IL). The difference between two groups was considered to be statistically significant at $P < 0.01$.

Results and discussion

Scheme 1A shows the process for preparation of the CP-pDNA nanoparticle microemulsion. The resulting microemulsion was stirred for a further 10 minutes until completely translucent. This procedure was used to prevent particle nucleation and growth inhibition. Thereafter, the CP-pDNA nanoparticles were isolated from the microemulsion according to a method modified from a published report,[29] which used van der Waals chromatography via HPLC (vdW-HPLC laundering) to produce stable, nonagglomerated, concentrated particles (as shown in Scheme 1B). We introduced vdW-HPLC laundering to isolate CP-pDNA nanoparticles via regulation of the electrostatic surface charges with the mobile phase solvent to inhibit or promote surface charging with nonpolar solvents and polar solvents. Ultraviolet HPLC was employed to elute and detect the CP-pDNA nanoparticles to identify whether they had eluted completely. The chromatography of the CP-pDNA nanoparticle

elution samples collected at different time points is shown in Figure 1B. The clear peaks of the CP-pDNA nanoparticles were detected in those samples eluted at 4, 8, and 10 hours. No signal was found from the sample eluted at 12 hours, indicating that the CP-pDNA nanoparticles were completely eluted from the silica column in 12 hours. The narrow peaks also indicated the homogeneity and purity of the CP-pDNA nanoparticles. The peaks appeared at almost the same time (approximately 13 minutes) when the extraction solvent (ethanol/water, volume ratio 70:30) with NaCl (5×10^{-4} M, prepared with CO_2 free deionized water, pH 7) was being pumped at 0.5 mL/minute. Absolute ethanol, the nonpolar solvent, inhibits the surface charge to permit attractive van der Waals forces to dominate and achieve reversible particle deposition onto the stationary phase. By maintaining this nonpolar environment, the weakly attracted organic molecules, such as plasmid DNA, Igepal CO-520, and cyclohexane, can be flushed through the column while the CP-pDNA nanoparticles remain adhered. After the materials including free plasmid DNA, Igepal 520, and cyclohexane were virtually removed (the remaining amounts were below the detection limits of ultraviolet HPLC analysis), the washing solvent was shifted to a solution with more polarity, namely, ethanol/water (v/v 70:30) with NaCl (5×10^{-4} M), which was prepared with CO_2 free deionized water (pH 7.0). In this situation, the surface charge on both the stationary phase and the CP-pDNA nanoparticles possessed significant electrosteric repulsion
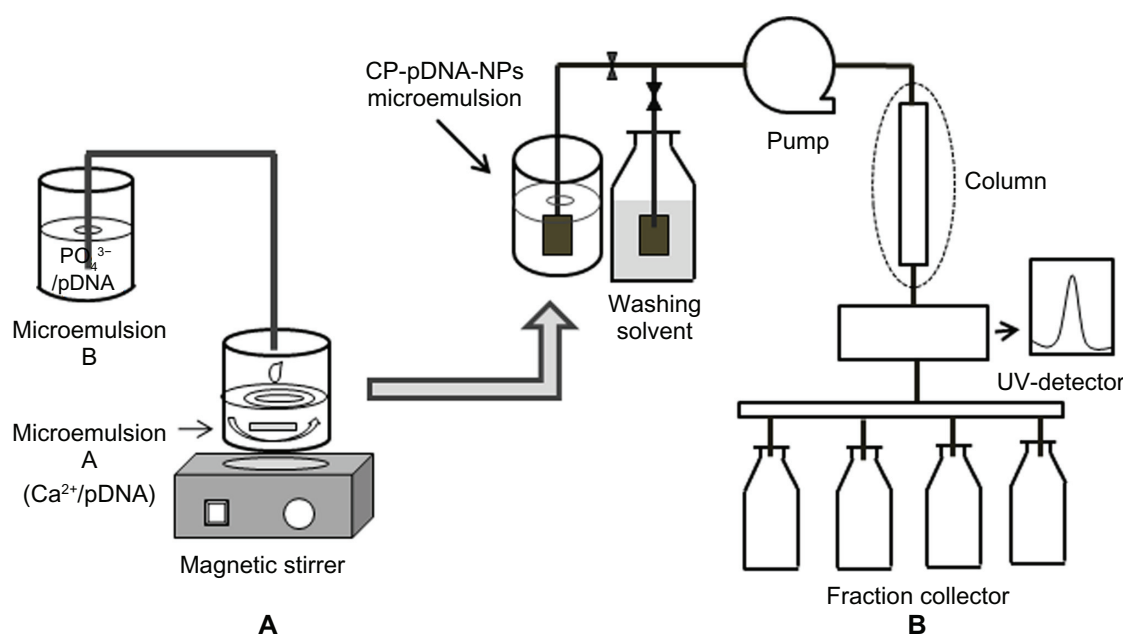

Scheme I (**A**) Process of preparing CP-pDNA nanoparticles by adding microemulsion B into microemulsion A at 20 drops per minute. (**B**) Schematic setup of the high-pressure liquid chromatography system for isolation of CP-pDNA nanoparticles.
Abbreviations: CP, calcium phosphate; pDNA, plasmid DNA.

to overcome the van der Waals attractive forces. During this process, the Cl⁻ provided assistance for the CP-pDNA nanoparticles to release from the column and elute. Finally, the eluted CP-pDNA nanoparticle solution was concentrated to obtain a well dispersed CP-pDNA nanoparticle solution.

Panel a of Figure 1C displays the optimized plasmid DNA loading capacity of the calcium phosphate nanoparticles via agarose gel electrophoresis, in which different amounts of TGF-β1 DNA (from 0.1 to 10 μg) were used to prepare the CP-pDNA nanoparticle microemulsions, while the same amounts of calcium and phosphate ions (1 μg) were used for different preparations. From the results of the gel electrophoresis (panel a of Figure 1C), we observed that 2:1 was the optimized weight ratio of calcium phosphate to plasmid DNA, indicating that the optimized loading capacity of plasmid DNA in the total CP-pDNA nanoparticles was approximately 33% (w/w). This loading capacity is significantly higher than that of the lipid-coated nano-calcium phosphate lipid/DNA weight ratio of 10:1 stated in one published report.[36] To confirm the integrity of the plasmid DNA incorporated into the nanoparticles, SmaI digestion of plasmid DNA released from the CP-pDNA nanoparticles was performed. Panel b of Figure 1C demonstrates the gel electrophoresis results of the TGF-β1 plasmid DNA cut into three fragments (approximately 4.5 kb, 2.5 kb, and 0.6 kb) by SmaI digestion, ie, the plasmid DNA recovered from the CP-pDNA nanoparticles shows the same digestion pattern as that of free plasmid DNA. In addition, no smears were observed on the recovered plasmid DNA. Therefore, the plasmid DNA encapsulated in CP-pDNA nanoparticles was intact, which suggests that the integrity of the plasmid TGF-β1 in the CP-pDNA nanoparticles was maintained. Panel c of Figure 1C reveals that plasmid DNA encapsulated into the calcium phosphate nanoparticle could still keep the supercoiled conformation. Moreover, calcium concentrations had no effect on the topological structure of plasmid DNA since there were no obvious changes observed in the intensity of fluorescence strips from different lines (panel c of Figure 1C).

TEM images were taken with a JEM-2100 instrument for CP-pDNA nanoparticles prepared with different weight ratios of calcium phosphate to plasmid DNA (0.1:1, 0.5:1, 1:1, 2:1, 5:1, and 10:1; panels a–f of Figure 2A). There was no significant size variation between the different preparations, but when the calcium phosphate to plasmid DNA weight ratio increased to 10:1, the particle size distribution became extremely nonuniform. The CP-pDNA nanoparticles prepared at a 2:1 ratio were monodispersed, and their diameters were further characterized. The average diameter of the CP-pDNA
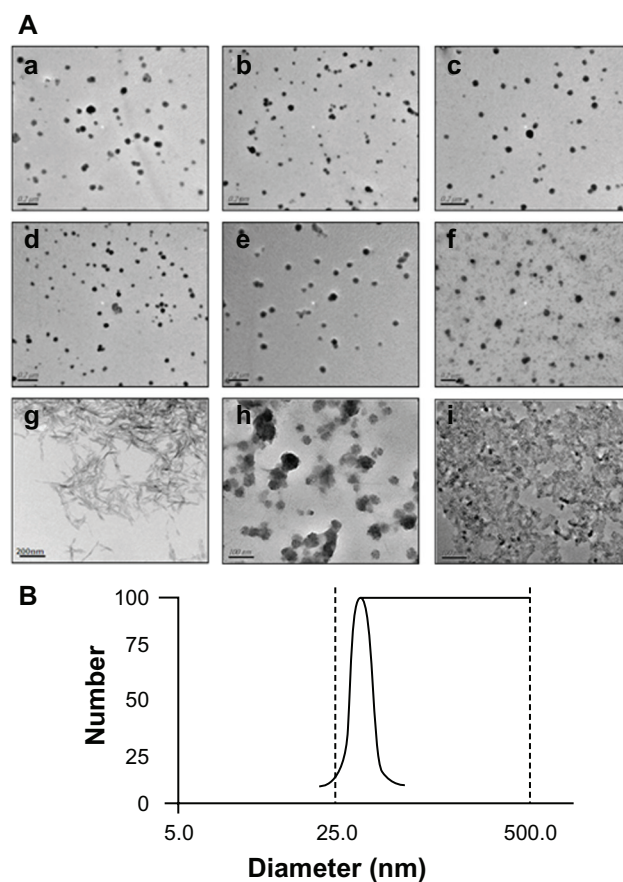
Figure 2 (**A**) Transmission electron microscopy images. Panels a–f show CP-pDNA nanoparticles made with calcium phosphate/plasmid DNA ratios equal to 0.1:1 (a), 0.5:1 (b), 1:1 (c), 2:1 (d), 5:1 (e), and 10:1 (f); panel g shows needle-like calcium phosphate particles. Panels h and i show the standard calcium phosphate transfection agent. Panel h shows quiescence at 0.5 hours; panel i shows quiescence at 8 hours. (**B**) Particle size distribution of CP-pDNA nanoparticles made with a calcium phosphate/plasmid DNA ratio of 2:1.
Abbreviations: CP, calcium phosphate; pDNA, plasmid DNA.

nanoparticles was approximately 20–50 nm with a spherical shape (panel e of Figure 2A), based on the measurements of 150 nanoparticles in the TEM photomicrographs. The particle size distribution was measured at a calcium phosphate to plasmid DNA weight ratio of 2:1, demonstrating that the CP-pDNA nanoparticle diameters ranged from 25 nm to 50 nm (Figure 2B), which was consistent with the findings of TEM (panel e of Figure 2A). The CP-pDNA nanoparticles with this small and uniform particle size, which was comparable with or even smaller than that of previous studies,[25,31] were well dispersed without any sign of agglomeration. Small size and effective dispersion contribute greatly to transfection efficiency.

Mesenchymal stem cells have been widely investigated for use in gene therapies.[33] In this study, we isolated mesenchymal stem cells from the tibia and the femur of one-day-old male white Sprague-Dawley rats. Passage 3 rat mesenchymal
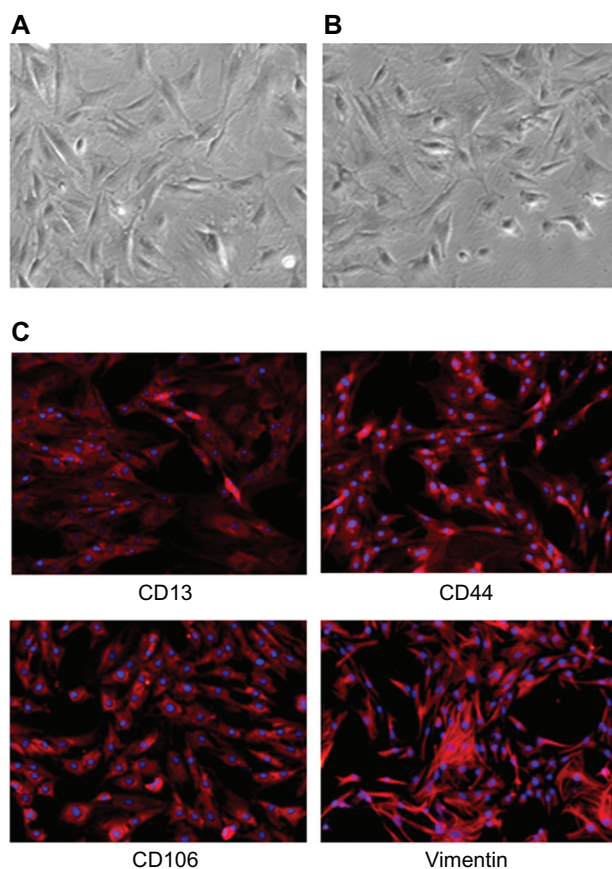
stem cells appeared fibroblastic and homogeneous in size and morphology before transfection, as shown in Figure 3A. Figure 3B shows the fibroblastic appearance of the stem cells after transfection. Immunofluorescence staining showed that the rat mesenchymal stem cells were positive for CD13, CD44, CD106, and vimentin, as revealed by red fluorescence (Figure 3C), and negative for CD34 and CD71 (data not shown). For immunofluorescence analysis, rabbit antimouse antibodies, CD13, CD44, CD106, CD34, CD71, and vimentin, were used as the primary antibodies, and Cy3-conjugated sheep antirabbit IgG was employed as the secondary antibody. CY3 is a type of biological fluorescent dye, which is activated by laser light at the wavelength of 554 nm and emits fresh red fluorescence within the wavelength range of 568–574 nm. Thus, Cy3-conjugated sheep antirabbit IgG combined with the primary antibodies (rabbit antimouse antibodies CD13, CD44, CD106, and vimentin) showed red fluorescence (Figure 3C), indicating the presence of the surface markers, CD13, CD44, CD106, and vimentin, respectively. However, no fluorescence was observed in the

Figure 3 (**A**) Mesenchymal stem cells before transfection. (**B**) Mesenchymal stem cells after transfection. (**C**) Surface markers used to identify mesenchymal stem cells; CD13, CD44, CD106, and vimentin were all positive, as revealed by red fluorescence.

CD34 and CD71 groups. This indicates that the mesenchymal lineage surface markers were present in the cultures and that hematopoietic cell markers were not. Therefore, based on morphology and surface markers, the cultured cells were probably mesenchymal stem cells.[33,37] Furthermore, the same results were obtained after transfection, indicating that the stem cells had not differentiated following transfection.
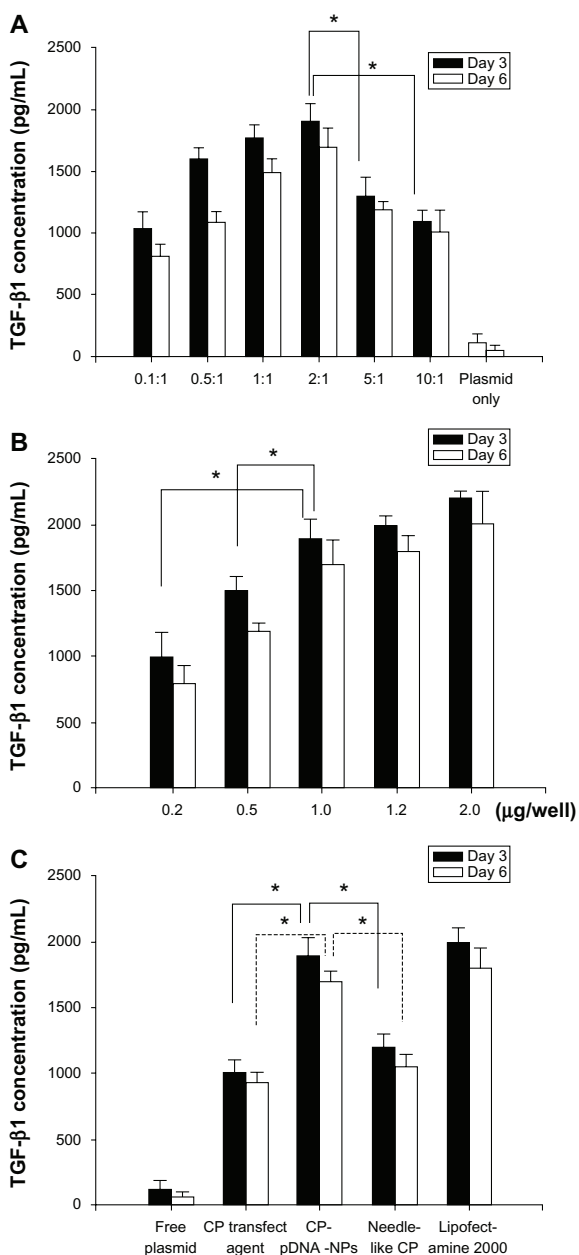
Plasmid TGF-β1 was used as an exogenous gene to transfect the mesenchymal stem cells. TGF-β1 is a member of a large family of structurally related peptides that plays a key role in regulating cell proliferation, differentiation, apoptosis, and production of extracellular matrix.[38] It has been reported that TGF-β1 is an effective stimulator of chondrogenesis in mesenchymal stem cells.[39] Thus, the overexpression of TGF-β1 in mesenchymal stem cells could be used in cartilage tissue regeneration. We believe that with development in research, the expression of TGF-β1 could be used in other types of tissue regeneration.

Herein, mesenchymal stem cells were used in gene transfection experiments. The optimized phosphate/pDNA ratio during CP-pDNA nanoparticle preparation, which displayed highest transfection efficiency for mesenchymal stem cells in vitro at day 3 and day 6, was 2:1 (Figure 4A). There was an approximately 18-fold elevation in TGF-β1 expression in the mesenchymal stem cells treated with CP-pDNA nanoparticles prepared at a 2:1 ratio compared with those from the control groups treated with plasmid only. In all of the subsequent studies, CP-pDNA nanoparticles were prepared at a 2:1 ratio. The most suitable dose of CP-pDNA nanoparticles for transfection was 1 μg, as demonstrated in the dose-response assay (Figure 4B).

For comparison with our CP-pDNA nanoparticles, the transfection efficiencies of a standard Lipofectamine 2000 method, a standard calcium phosphate transfection method, and a method in which plasmid DNA was mixed with preformed needle-like calcium phosphate nanoparticles were tested. According to the method reported by Lai et al,[40] in which the resulting particle was approximately 4–8 nm in diameter and approximately 80–100 nm in length, we also prepared needle-like calcium phosphate nanoparticles approximately 10–20 nm in diameter and approximately 100–120 nm in length (panel g of Figure 2A. As shown in Figure 4C, there was no significant difference between the TGF-β1 expression levels of the mesenchymal stem cells transfected with our CP-pDNA nanoparticles and the same amount of plasmid mediated by Lipofectamine 2000. As expected, the transfection efficiency of our CP-pDNA nanoparticles was significantly higher than those

Figure 4C, the lower cytotoxicity reveals the superior results using CP-pDNA nanoparticles (Figure 5A). The CP-pDNA nanoparticles prepared in this study showed other excellent advantages, such as ultralow particle size (approximately 20–50 nm), spherical shape, effective dispersion, and
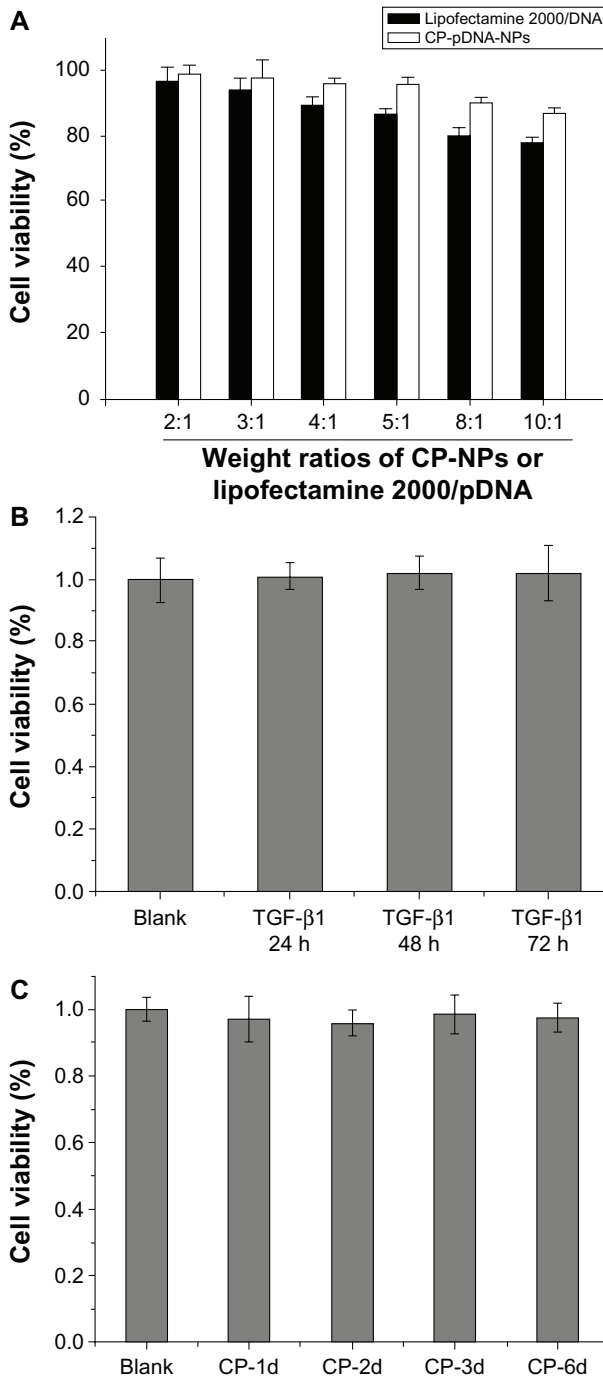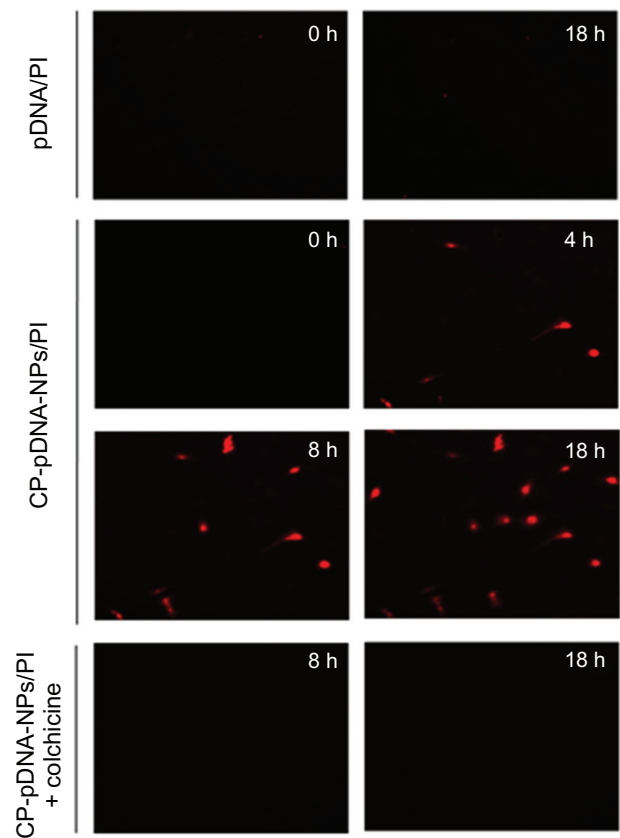

Figure 4 TGF-β1 expression. (**A**) Mesenchymal stem cells transfected with CP-pDNA nanoparticles made at different calcium phosphate/pDNA ratios (0.1:1 to 10:1). (**B**) Mesenchymal stem cells transfected with different amounts (0.2 μg to 2.0 μg) of CP-pDNA nanoparticles (2:1 was used for the calcium phosphate/pDNA ratio). The enzyme-linked immunosorbent assay results from day 3 are shown with black bars, and those from day 6 are shown with white bars. (**C**) TGF-β1 expression levels from mesenchymal stem cells transfected with plasmid DNA using different approaches. The enzyme-linked immunosorbent assay results from day 3 are shown with black bars, and those from day 6 are shown with white bars (*$P < 0.05$, Student's *t*-test).
Abbreviations: TGF-β1, transforming growth factor beta-1; CP, calcium phosphate; pDNA, plasmid DNA.

of the standard calcium phosphate transfection ($P < 0.01$, Student's *t*-test) and the needle-like calcium phosphate nanoparticles ($P < 0.01$, Student's *t*-test). Although the CP-pDNA nanoparticles demonstrated transfection efficiency comparable with that of Lipofectamine 2000, as shown in

Figure 5 Cytotoxicity assays. (**A**) Preparations with different weight ratios (2:1 to 10:1) of CP:pDNA or Lipofectamine 2000:pDNA. (**B**) Cytotoxicity of plasmid TGF-β1 at the concentration of 200 ng/well. Viability of cells was analyzed 3 days after the transfection. (**C**) Cytotoxicity of CP to mesenchymal stem cells up to 6 days.
**Abbreviations:** TGF-β1, transforming growth factor beta-1; CP, calcium phosphate.

maintenance of the integrity of the plasmid encapsulated in the calcium phosphate nanocomposite particles. Effective dispersion is prerequisite for the ultralow size and large contact surface which result in enhanced cellular uptake. Aside from particle size, particle morphology also greatly affects gene transfection.[35] However, needle-like calcium phosphate particles, unlike spherical CP-pDNA nanoparticles, are relatively difficult for cells to take up.[41,42] This difficulty may possibly be because the shape of needle-like calcium phosphate particles is unfavorable for endocytosis. A more exact explanation will be addressed in our future work. In the case of standard calcium phosphate, agglomeration caused lower transfection efficiency because severe agglomeration was observed after 8 hours of static placing (panels h and i of Figure 2A). More importantly, these CP-pDNA nanoparticles have the capacity to keep encapsulated DNA intact during the entire process of CP-pDNA nanoparticle production, including the use of solvents such as cyclohexane and Igepal CO-520, and isolation through vdW-HPLC laundering and dialysis, which is another basic requirement leading to high transfection efficiency. All of these factors greatly affect the process of cellular uptake and increase the transfection efficiency. Additionally, plasmid TGF-β1 at the concentration used in this study (200 ng/well) was nontoxic to mesenchymal stem cells, as shown in Figure 5B. Furthermore, the toxicity of calcium phosphate to mesenchymal stem cells was also investigated during chronic exposure for up to 6 days, and the results show that calcium phosphate was not toxic to mesenchymal stem cells, as shown in Figure 5C.

Live cell imaging was used to investigate the transportation process of CP-pDNA nanoparticles in mesenchymal stem cells. Propidium iodide was used as a marker for plasmid DNA. The propidium iodide molecules were bound to plasmid DNA and incorporated into the nanoparticles during preparation. The cells in which foreign plasmid DNA had accumulated could be detected as red fluorescence. The CP-pDNA/propidium iodide nanoparticle-transfected mesenchymal stem cells were continuously observed under a live cell image system for 18 hours. Representative images at 0, 4, 8, and 18 hours after transfection are shown in the middle panels of Figure 6. Generally, red fluorescence was detected in a few cells by 4 hours after transfection. At the beginning (0 hours), no red fluorescence was observed in any of the tested groups (Figure 6). However, over time, red fluorescence spots increasingly appeared in the CP-pDNA nanoparticle group, and images were taken in the same field of view. That is, images in the same group were pictures of the same cells taken at different time points. The number of

Figure 6 Live cell images of mesenchymal stem cells for 18 hours after transfection with propidium iodide (PI)-labeled free plasmid DNA, propidium iodide-labeled CP-pDNA nanoparticles and propidium iodide-labeled CP-pDNA nanoparticles added with colchicine. The images of the same cells at different time points were shown.
Abbreviations: CP, calcium phosphate; pDNA, plasmid DNA.

cells turning red gradually increased until 18 hours. In the absence of calcium phosphate, free DNA plasmids could not enter the mesenchymal stem cells (upper panels in Figure 6). The same situation occurred with mesenchymal stem cells transfected with CP-pDNA nanoparticles/propidium iodide added with colchicine (lower panels in Figure 6). Colchicine is a widely used endocytosis inhibitor[43,44] that can effectively inhibit endocytosis in a cell membrane, as shown by the significantly reduced red fluorescence observed in the lower panels of Figure 6. The increasing intensive red fluorescence in the CP-pDNA nanoparticle group indicated that an increasing amount of plasmid DNA was transported into the cytoplasm. A previous study has confirmed that calcium phosphate is taken up by endocytosis, dissolved in acidic compartments (for example, endosomes and lysosomes), and subsequently released into the cytoplasm.[45] The results illustrated by the lower panels of Figure 6 also confirm that CP-pDNA nanoparticles were transported by the cell endocytosis pathway. Once propidium iodide was released into cytoplasm, it could combine with the large amount of DNA
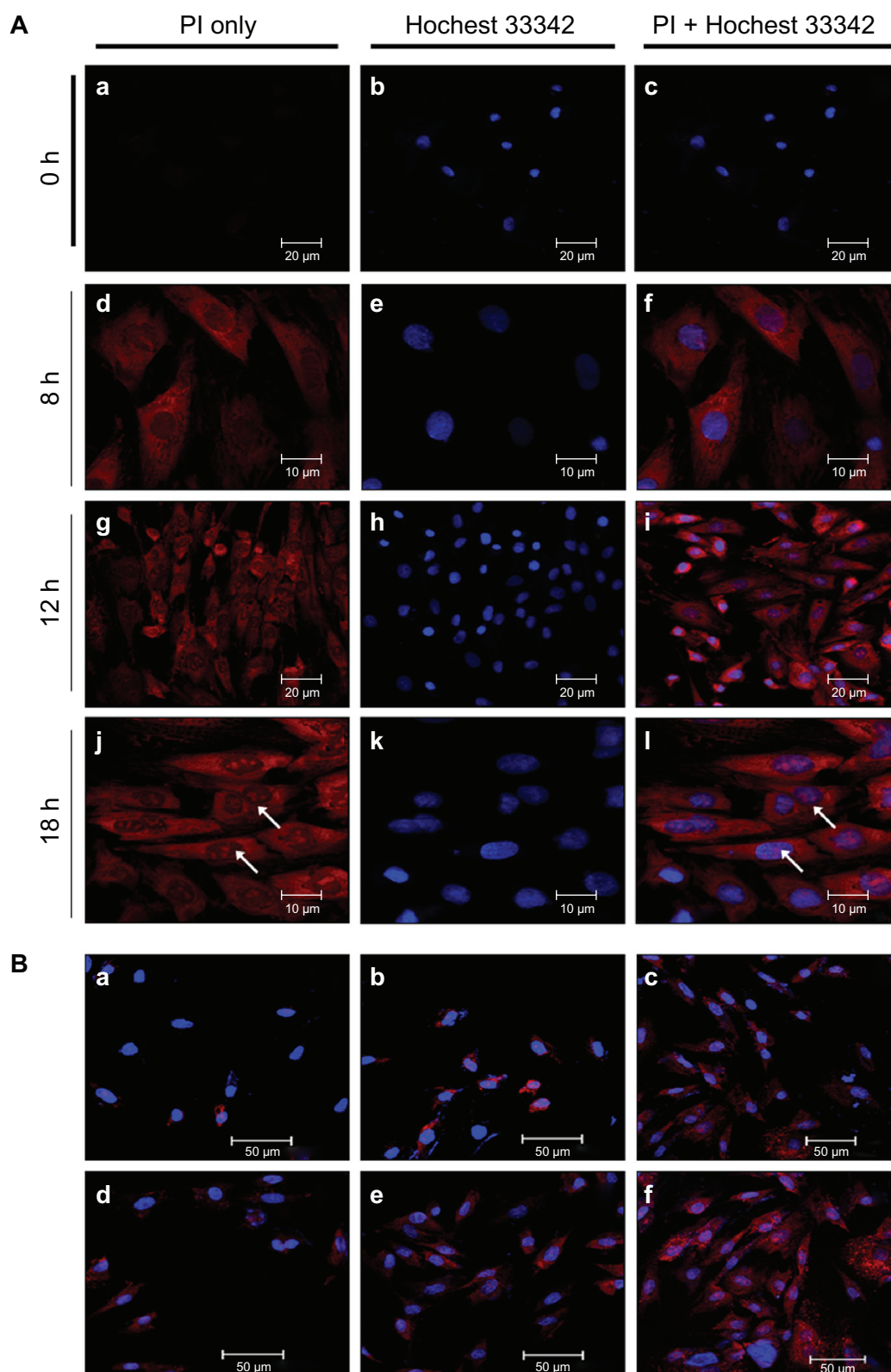
Figure 7 (**A**) Real-time imaging of CP-pDNA/propidium iodide (PI) nanoparticles after transfecting mesenchymal stem cells. First column, panels a, d, g and j show mesenchymal stem cells stained with propidium iodide only at 0, 8, 12, and 18 hours after transfection, respectively; second column, panels b, e, h and k show mesenchymal stem cells stained with Hoechst 33342 only at 0, 8, 12, and 18 hours after transfection, respectively; third column, panels c, f, i, and l show mesenchymal stem cells stained with both propidium iodide and Hoechst 33342 at 0, 8, 12, and 18 hours after transfection, respectively. (**B**) Confocal laser microscopy images of mesenchymal stem cells. Panels a, b, c show mesenchymal stem cells at 18 hours after transfection using needle-like calcium phosphate nanoparticles, standard calcium phosphate transfection, and Lipofectamine 2000, respectively; panels d, e, and f show mesenchymal stem cells at 4, 8, and 18 hours after transfection using CP-pDNA/propidium iodide nanoparticles.
Abbreviations: CP, calcium phosphate; pDNA, plasmid DNA.

originally existing inside the mesenchymal stem cells, and thus markedly red fluorescence was observed, as shown in the group of mesenchymal stem cells transfected with CP-pDNA nanoparticles/propidium iodide (middle panels of Figure 6).

Laser confocal fluorescence microscopy was used to track the subcellular positions of CP-pDNA nanoparticles/propidium iodide. Hoechst 33342 was used to show the positions of the nuclei, and propidium iodide was used to track the plasmid DNA. Figure 7A shows the CP-pDNA nanoparticle transportation process in the mesenchymal stem cells at 0, 8, 12, and 18 hours after transfection. After 12 hours of transfection, plasmid DNA was clearly observed in the cytoplasm, and at 18 hours, plasmid DNA was clearly observed in the nuclei, demonstrating that CP-pDNA nanoparticles could successfully deliver foreign DNA into mesenchymal stem cell nuclei to ensure expression of therapeutic nucleic acids. The CP-pDNA nanoparticles entered the cell by endocytosis. To prevent degradation, the CP-pDNA nanoparticles should escape the endosome before its fusion with lysosomes. The low pH established in the lysosomes leads to dissolution of calcium phosphate and release of DNA. Nevertheless, Maitra[46] found that partial dissolution of calcium phosphate can destabilize the lysosomal membrane and facilitate release of the remaining nanoparticles and plasmid DNA into the cytoplasm. Thereafter, the plasmid DNA will move toward the nucleus.[47] It is still unknown whether CP-pDNA nanoparticles penetrate the nuclear membrane or enter the nucleus during mitosis or other cell cycle periods. Further investigation concerning the mechanism of cellular uptake will be conducted in our future work.

The mesenchymal stem cells transfected with CP-pDNA/propidium iodide nanoparticles were compared with those achieved using other methods (for example, needle-like calcium phosphate nanoparticles, a standard calcium phosphate transfection kit, and Lipofectamine 2000). At 18 hours after transfection, plasmid DNA were abundantly distributed in mesenchymal stem cells transfected with CP-pDNA nanoparticles or Lipofectamine 2000 methods, while much less was observed in those transfected with needle-like calcium phosphate nanoparticles or the standard calcium phosphate transfection kit (panels a, b, c, and f in Figure 7B). Plasmid DNA could be clearly observed in the nuclei of mesenchymal stem cells transfected with the CP-pDNA nanoparticles and Lipofectamine 2000 (panels c and f in Figure 7B, shown using arrows). Notably, it seems that the CP-pDNA nanoparticle method provides more rapid transportation of plasmid DNA than does Lipofectamine 2000. Eight hours after CP-pDNA

nanoparticle transfection, approximately the same plasmid DNA abundance was seen in the mesenchymal stem cells as seen 18 hours after Lipofectamine 2000-mediated transfection (panels e and c in Figure 7B). This result indicates that TGF-β1 transfected by CP-pDNA nanoparticles might take less time to reach a sufficient expression level.

Conclusion

The CP-pDNA nanoparticles that have been constructed in this study had such advantages as ultralow particle size (20 nm) and excellent dispersity, in addition to an ability to keep encapsulated DNA intact. The TGF-β1 plasmid was successfully encapsulated into calcium phosphate nanoparticles with a relatively large loading capacity (the weight ratio of plasmid DNA in the total CP-pDNA nanoparticles was approximately 33%). Interestingly, the SmaI digestion assay revealed that the plasmid TGF-β1 in the CP-pDNA nanoparticles was intact after all of these production processes. The results of immunofluorescence staining showed the presence of mesenchymal lineage cell surface markers, CD13, CD44, CD106, and vimentin, and the absence of hematopoietic markers, CD34 and CD71, indicating that the cells cultured were likely mesenchymal stem cells. After transfection, the stem cells had not differentiated. Compared with Lipofectamine 2000-mediated transfection, the cytotoxicity of CP-pDNA nanoparticles was significantly lower when the CP-pDNA nanoparticles or Lipofectamine 2000 to plasmid DNA weight ratios increased to 5:1, 8:1, or 10:1, which demonstrated that the CP-pDNA nanoparticles were safe as gene vectors. Both plasmid TGF-β1 and calcium phosphate were not toxic to the mesenchymal stem cells. Most importantly, the transfection efficiency of the CP-pDNA nanoparticles was comparable with that of Lipofectamine 2000, but it was significantly higher than that of standard calcium phosphate transfection ($P < 0.01$, Student's t-test) and use of needle-like calcium phosphate nanoparticles ($P < 0.01$, Student's t-test). This study represents considerable progress in the use of calcium phosphate particles as nonviral gene vectors. In general, CP-pDNA nanoparticles appear to be a promising candidate as a nonviral gene vector in gene therapy and tissue engineering.

Acknowledgments

The authors also thank the University Ethics Committee for its kind guidance with the animal experiments.

Disclosure

The authors report no conflicts of interest in this work.

References

1. Niidome T, Huang L. Gene therapy progress and prospects: nonviral vectors. *Gene Ther*. 2002;9:1647–1652.
2. Karmakar A, Bratton SM, Dervishi E, et al. Ethylenediamine functionalized-single-walled nanotube (f-SWNT)-assisted in vitro delivery of the oncogene suppressor p53 gene to breast cancer MCF-7 cells. *Int J Nanomed*. 2011;6:1045.
3. Prud'homme G, Draghia-Akli R, Wang Q. Plasmid-based gene therapy of diabetes mellitus. *Gene Ther*. 2007;14:553–564.
4. Mátrai J, Chuah M, Vandendriessche T. Preclinical and clinical progress in hemophilia gene therapy. *Curr Opin Hematol*. 2010;17:387–392.
5. Feng M, Lee D, Li P. Intracellular uptake and release of poly (ethyleneimine)-co-poly (methyl methacrylate) nanoparticle/pDNA complexes for gene delivery. *Int J Pharm*. 2006;311:209–214.
6. Oligino TJ, Yao Q, Ghivizzani SC, Robbins P. Vector systems for gene transfer to joints. *Clin Orthop*. 2000;379:S17–S30.
7. McMenamin M, Wood M. Progress and prospects: Immunobiology of gene therapy for neurodegenerative disease: prospects and risks. *Gene Ther*. 2010;17(4):448–458.
8. Luo D, Saltzman WM. Synthetic DNA delivery systems. *Nat Biotechnol*. 2000;18:33–37.
9. Hu Q, Zuo P, Shao B, et al. Administration of nonviral gene vector encoding rat β-defensin-2 ameliorates chronic Pseudomonas aeruginosa lung infection in rats. *Gene Med*. 2010;12:276–286.
10. Corsi K, Chellat F, Yahia LH, Fernandes JC. Mesenchymal stem cells, MG63 and HEK293 transfection using chitosan-DNA nanoparticles. *Biomaterials*. 2003;24:1255–1264.
11. Han G, You C, Kim B, et al. Light-regulated release of DNA and its delivery to nuclei by means of photolabile gold nanoparticles. *Angew Chem Int Ed Engl*. 2006;45:3165–3169.
12. Thomas M, Klibanov AM. Conjugation to gold nanoparticles enhances polyethylenimine's transfer of plasmid DNA into mammalian cells. *Proc Natl Acad Sci U S A*. 2003;100:9138–9143.
13. Giri S, Trewyn BG, Stellmaker MP, Lin VSY. Stimuli-responsive controlled-release delivery system based on mesoporous silica nanorods capped with magnetic nanoparticles. *Angew Chem Int Ed Engl*. 2005;44:5038–5044.
14. Xu ZP, Zeng QH, Lu GQ, Yu AB. Inorganic nanoparticles as carriers for efficient cellular delivery. *Chem Eng Sci*. 2006;61:1027–1040.
15. Sokolova V, Epple M. Inorganic nanoparticles as carriers of nucleic acids into cells. *Angew Chem Int Ed Engl*. 2008;47:1382–1395.
16. Son SJ, Bai X, Lee SB. Inorganic hollow nanoparticles and nanotubes in nanomedicine Part 1. Drug/gene delivery applications. *Drug Discov Today*. 2007;12:650–656.
17. Wang S, McDonnell EH, Sedor FA, Toffaletti JG. pH effects on measurements of ionized calcium and ionized magnesium in blood. *Arch Pathol Lab Med*. 2002;126:947–950.
18. Yih TC, Al-Fandi M. Engineered nanoparticles as precise drug delivery systems. *J Cell Biochem*. 2006;97:1184–1190.
19. Graham F, Van der Eb A. A new technique for the assay of infectivity of human adenovirus 5 DNA. *Virology*. 1973;52:456–467.
20. Liu YC, Wang T, He FL, et al. An efficient calcium phosphate nanoparticle-based non-viral vector for gene delivery. *Int J Nanomed*. 2011;6:721–727.
21. Olton D, Li J, Wilson ME, et al. Nanostructured calcium phosphates (NanoCaPs) for non-viral gene delivery: Influence of the synthesis parameters on transfection efficiency. *Biomaterials*. 2007;28:1267–1279.
22. Sokolova VV, Radtke I, Heumann R, Epple M. Effective transfection of cells with multi-shell calcium phosphate-DNA nanoparticles. *Biomaterials*. 2006;27:3147–3153.
23. Roy I, Mitra S, Maitra A, Mozumdar S. Calcium phosphate nanoparticles as non-viral vectors for targeted gene delivery. *Int J Pharm*. 2003;250:25–33.
24. Bisht S, Bhakta G, Mitra S, Maitra A. pDNA loaded calcium phosphate nanoparticles: highly efficient non-viral vector for gene delivery. *Int J Pharm*. 2005;288:157–168.
25. Liu T, Tang AF, Zhang GY, et al. Calcium phosphate nanoparticles as a novel non-viral gene vector for efficient transfection of DNA in cancer therapy. *Cancer Biother Radiopharm*. 2005;20:141–149.
26. Zhang MZ, Ishii A, Nishiyama N, et al. PEGylated calcium phosphate nanocomposites as smart environment-sensitive carriers for siRNA delivery. *Adv Mater*. 2009;21:3520–3525.
27. Krebs MD, Salter E, Chen E, Sutter KA, Alsberg E. Calcium phosphate-DNA nanoparticles gene delivery from alginate hydrogels induces *in vivo* osteogenesis. *J Biomed Mater Res A*. 2010;92A:1131–1138.
28. Keeney M, Van Den Beucken JJJP, Van Der Kraan PM, Jansen JA, Pandit A. The ability of a collagen/calcium phosphate scaffold to act as its own vector for gene delivery and to promote bone formation via transfection with VEGF165. *Biomaterials*. 2010;31:2893–2902.
29. Morgan TT, Muddana HS, Altinoglu EI, et al. Encapsulation of organic molecules in calcium phosphate nanocomposite particles for intracellular imaging and drug delivery. *Nano Lett*. 2008;8:4108–4115.
30. Pedraza CE, Bassett DC, McKee MD, Nelea V, Gbureck U, Barralet JE. The importance of particle size and DNA condensation salt for calcium phosphate nanoparticle transfection. *Biomaterials*. 2008;29:3384–3392.
31. Kester M, Heakal Y, Fox T, et al. Calcium phosphate nanocomposite particles for in vitro imaging and encapsulated chemotherapeutic drug delivery to cancer cells. *Nano Lett*. 2008;8:4116–4121.
32. Muddana HS, Morgan TT, Adair JH, Butler PJ. Photophysics of Cy3-encapsulated calcium phosphate nanoparticles. *Nano Lett*. 2009;9:1559–1566.
33. Alhadlaq A, Mao JJ. Mesenchymal stem cells: isolation and therapeutics. *Stem Cells Dev*. 2004;13:436–448.
34. Elisseeff J, McIntosh W, Fu K, Blunk T, Langer R. Controlled-release of IGF-I and TGF-β1 in a photopolymerizing hydrogel for cartilage tissue engineering. *J Orthop Res*. 2001;19:1098–1104.
35. Orrantia E, Chang PL. Intracellular distribution of DNA internalized through calcium phosphate precipitation. *Exp Cell Res*. 1990;190:170–174.
36. Zhou C, Yu B, Yang X, et al. Lipid-coated nano-calcium-phosphate (LNCP) for gene delivery. *Int J Pharm*. 2010;392:201–208.
37. Jiang WH, Ma AQ, Wang TZ, et al. Homing and differentiation of mesenchymal stem cells delivered intravenously to ischemic myocardium in vivo: a time-series study. *Pflugers Arch Eur J Physiol*. 2006;453:43–52.
38. Zhang YF, Cheng XR, Wang JW, et al. Novel chitosan/collagen scaffold containing transforming growth factor-β1 DNA for periodontal tissue engineering. *Biochem Biophys Res Commun*. 2006;344:362–369.
39. Guo CA, Liu XG, Huo JZ, Jiang C, Wen XJ, Chen ZR. Novel gene-modified-tissue engineering of cartilage using stable transforming growth factor-β1-transfected mesenchymal stem cells grown on chitosan scaffolds. *J Biosci Bioeng*. 2007;103:547–556.
40. Lai C, Tang SQ, Wang YJ, Wei K. Formation of calcium phosphate nanoparticles in reverse microemulsions. *Mater Lett*. 2005;59:210–214.
41. Jordan M, Wurm F. Transfection of adherent and suspended cells by calcium phosphate. *Methods*. 2004;33:136–143.
42. Liu X, Qin D, Cui Y, et al. The effect of calcium phosphate nanoparticles on hormone production and apoptosis in human granulosa cells. *Reprod Biol Endocrinol*. 2010;8:32.
43. Kitchens KM, Kolhatkar RB, Swaan PW, Ghandehari H. Endocytosis inhibitors prevent poly (amidoamine) dendrimer internalization and permeability across Caco-2 cells. *Mol Pharm*. 2008;5:364–369.

44. Liu Y, Huang R, Han L, et al. Brain-targeting gene delivery and cellular internalization mechanisms for modified rabies virus glycoprotein RVG29 nanoparticles. *Biomaterials*. 2009;30:4195–4202.

45. Neumann S, Kovtun A, Dietzel ID, Epple M, Heumann R. The use of size-defined DNA-functionalized calcium phosphate nanoparticles to minimise intracellular calcium disturbance during transfection. *Biomaterials*. 2009;30:6794–6802.

46. Maitra A. Calcium-phosphate nanoparticles: second-generation nonviral vectors in gene therapy. *Expert Rev Mol Diagn*. 2005;5: 893–905.

47. Loyter A, Scangos G, Juricek D, Keene D, Ruddle F. Mechanisms of DNA entry into mammalian cells. II. Phagocytosis of calcium phosphate DNA co-precipitate visualized by electron microscopy. *Exp Cell Res*. 1982;139:223–234.